FRACTURE TOUGHNESS TESTS ON PLASMA-SPRAYED COATINGS

C. C. Berndt

NASA-Lewis Research Center, MS 105-1, Cleveland, OH 44135, USA

ABSTRACT

Fracture toughness measurements have been performed on plasma-sprayed coatings. The intrinsic fracture toughness of plasma-sprayed coatings may be ascertained by means of a double cantilever beam (DCB) test. Emphasis is placed on calibration of the specimen geometry. Representative values for alumina coatings are presented.

KEYWORDS

Plasma-sprayed coating, double cantilever beam, strain energy release rate, adhesion.

INTRODUCTION

It is difficult to measure the mechanical properties of plasma-sprayed coatings. There are a large number of destructive tests which may be used to determine the adhesion quality of plasma-sprayed coatings (Berndt and McPherson, 1979). They may be broadly classified as either tensile, shear, and fracture mechanics.

The tensile adhesion (or "bond strength") test is most frequently reported in the literature and is the method followed by the American Society for Testing and Materials (ASTM, 1969). A major problem is that the exact nature of the tensile forces can not be closely controlled and they do not necessarily reproduce the stress conditions which are imposed on the coating during its service life. This is usually manifested by a locus of failure which is unrepresentative of the usual service failure mode. There is also the more fundamental question of whether fracture strength, alone, can be attributable to the adhesion quality of the coating.

There is no standard method for carrying out shear tests and it is difficult to compare results from separate studies. The methods (Zakharov and colleagues, 1970; Suhara, Kitajima and Fukada, 1974) essentially involve applying a tangential force (i.e., parallel to the substrate surface) to

promote coating failure. A major limitation is that the locus of failure and hence the strength measurement is controlled by the geometrical arrangement of a bushing which transmits force to the coating. Another test (Rykalin and Kudinov, 1976) has measured the force to shear individual particles from a substrate with a micro-knife. These workers defined a strength parameter which related the extent of particle interface reaction to increasing particle pressures and temperatures which were experienced during coating deposition.

Fracture mechanics tests are dissimilar to the tests which have been described above because they are carried out under controlled test conditions. Therefore the shape of the load versus extension curve is of critical importance in determining the materials properties of coatings. It should be emphasized that the "strength parameter" in this case is either G_{1C} or K_{1C}. The determination of fracture toughness properties of a coating has the advantage of conveying important information about the mechanism(s) of failure (Berndt and McPherson, 1981). The present work describes DCB tests; the double torsion method met with limited success (Berndt and McPherson, 1980).

EXPERIMENTS

It is necessary to incorporate the plasma-sprayed coating into the configuration of a fracture mechanics specimen (Fig. 1); as has been done for thick films (Becher and Newell, 1977; Bascom and Bitner, 1977; Pabst and Elssner, 1980). The concept of a DCB configuration, which has previously been used to test adhesive joints (Mostovoy, Crosley and Ripling, 1967), was used. The specimen preparation has been described previously (Berndt and McPherson, 1980). Essentially the coating was deposited onto a grit blasted substrate of surface dimensions approximately 6mm x 156mm. This sample was bonded with a commercial epoxy (Araldite D with Hardener HY951) to a support bar of similar dimensions. The composite specimen was machined flat on both faces to remove features created during the epoxy-casting process. If necessary the specimen was grooved to promote different failure modes.
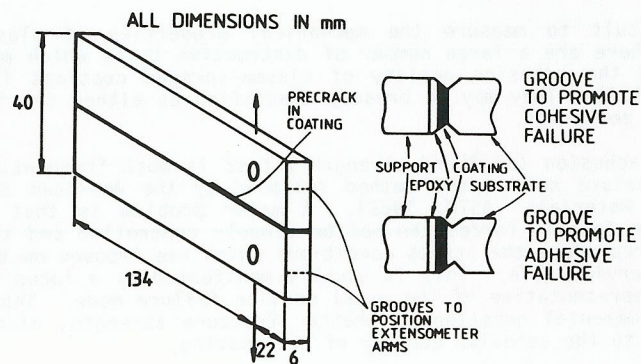

Fig. 1. DCB specimens used for compliance calibrations and fracture toughness testing of plasma-sprayed coatings.

The specimen was subjected to tensile forces through a clevis-pin arrangement and the extension measured with a strain gauge attached to the free ends of the DCB. In the following discussion the "loading point compliance" refers to measurements at the pins of the experimental arrangement (i.e., directly on the tensile axis). On the other hand the "extensometer compliance" was measured at the ends of the DCB where the extensometer was positioned. The total extension of the grip and specimen assembly could be measured by knowing the crosshead displacement rate and the time elapsed. Precracking was carried out with a jeweller's saw cut of width 0.2mm. It is crucial to point out that the deflection measured at the extensometer must be used in conjuction with a simple mathematical scaling expression to derive the displacement at the loading point.

RESULTS AND DISCUSSION

Development of Fracture Toughness Equation

The fracture toughness formulae that are used for DCB's must be modified since the extension was not measured at the tensile axis of the experimental arrangement. Figure 2 illustrates the types of DCB deformation that may be possible during a test and indicates that this modification to the fracture toughness formula also infers a specific model. For example the ratio of the extensometer to the loading point compliance is a constant for all crack lengths if the DCB deformation is described by Fig. 2a. That is:

$$\frac{\text{Extensometer Compliance}}{\text{Loading Point Compliance}} = \frac{C_E}{C_{LP}} = \frac{\text{total specimen length}}{\text{specimen length under load}} \quad (1)$$

$$= 156 / (156-22)$$

$$= 1.17$$

If the beams do not bend significantly (as shown in Fig. 2b) then the compliance ratio becomes;

$$\frac{C_E}{C_{LP}} = \frac{22 \times 10^{-3} + L}{L} \quad (2)$$

where   L = crack length (m)

The loading point compliance was directly measured by attaching an extensometer to fixtures which were aligned axially to the loading force. The deflection at the usual extensometer position on the ends of the DCB arms was simultaneously measured. Rotation and shear at the crack tip (Mostovoy, Crosley and Ripling, 1967) was minimized by manufacturing a mild steel specimen with no adhesive joint. A comparison of the compliance ratios for 4 artifical cracks is shown in Table 1 where the "theoretical value" is calculated from equation 2. Thus the modelling of DCB deformation, in this experimental case, is thought to incorporate bending of the DCB arms as shown in Fig.2c.
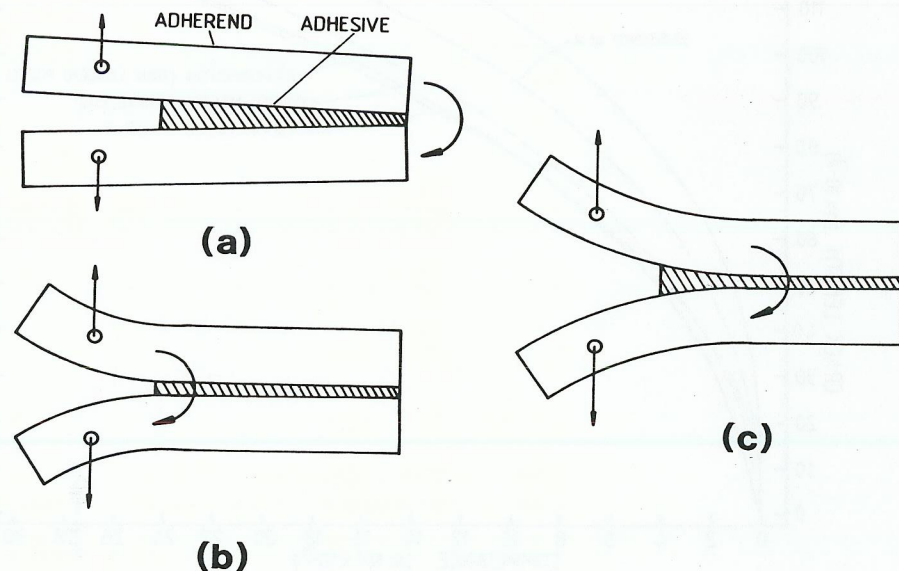
Fig. 2. Bending modes of DCB specimen.
(a) Rigid arms (equation 1).
(b) Cantilever beams originating at the crack tip (equation 2).
(c) Rotation of cantilever beams at a point beyond the crack tip.

TABLE 1. Compliance Ratio For 4 Crack Lengths

Crack Length $\times 10^{-3}$ m	C_E/C_{LP} theory	C_E/C_{LP} experimental
17.6	2.25	2.17
39.3	1.56	1.88
59.3	1.39	1.19
89.7	1.25	1.04

The extensometer compliance fitted an empirical equation

$$C_E = 2.108 \times 10^{-4} \times L^{1.989} \tag{3}$$

which showed a coefficient of variance of 0.99 over 57 trials (i.e., 57 artificial crack lengths) involving 4 calibration adhesive joints.

The critical strain energy release rate can be determined from

$$G_{1C} = \frac{P_c^2}{2W} \times \frac{dC}{dL} \tag{4}$$

where G_{1C} = critical strain energy release rate (J m^{-2})

   P_c = critical force (N)

   $\frac{dC}{dL}$ = specimen compliance change with crack length

On combining equations 2, 3 and 4 the coating fracture toughness may be evaluated from

$$G_{1C} = \frac{P_c^2}{12 \times 10^{-3}} \times \left\{ \frac{6.3 \times 10^{-4} \times L^{1.989}}{(22 \times 10^{-3} + L)} - \frac{2.108 \times 10^{-4} \times L^{2.989}}{(22 \times 10^{-3} + L)^2} \right\} \tag{5}$$

System Compliance

The extension between loading points may also be measured during a test from knowledge of the cross head speed (2.5×10^{-5} m min^{-1}) and the time elapsed. However a major complication arises because this measurement also incorporates deformation of the load train. Thus (Clausing, 1969)

$$C_T = C_G + C_{LP} \tag{6}$$

where C_T = total compliance

   C_G = grip compliance

   C_{LP} = load point compliance

A comparison of these system deformations is shown in Fig.3. The "load point compliance" of an uncracked specimen will approach zero so that C_G can be estimated as 2.75×10^{-7} m N^{-1} from Fig.3. The expression "E x W x C_G" where E is the Young's modulus and W is the specimen thickness, is a measure of rigidity for the load-train assembly. For the mild steel specimen used in this work: E x W x C_G = 280. A value of 600 is representative of a soft (load controlled) machine whereas a hard (displacement controlled) machine has a value of 1.5. In the case of these experiments the conditions are soft and the geometric stability factor varies from +5 to -5.

The compliance equation of Mostovoy and others (1967) may be generalized in the form $C = \frac{2}{3 \times E \times I} \times \left\{ (L + \alpha L_0)^3 + (\beta h^2 \times L) \right\}$ $\tag{7}$
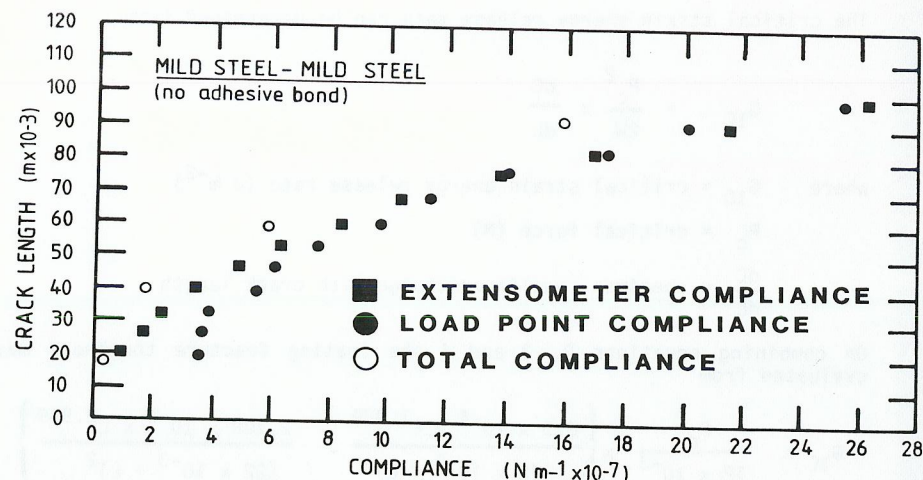
Fig. 3. Comparison of C_E, C_{LP} and C_T for a mild steel DCB specimen which does not incorporate an adhesive joint.

where
C	= compliance (mN^{-1})
L	= crack length (m)
E	= Young's modulus (Pa)
I	= moment of inertia of one cantilever arm (m^4)
h	= specimen height (m)
L_o	= offset of 0.6h due to beam rotation at the crack tip
h^2L	= correction for shear

The additional term " α " is an empirical constant which implies bending beyond the crack tip and " β " is another constant which accounts for displacement and shear at the crack tip. Several sets of data for this compliance relation with α =2 and β =2 or 6 are shown in Fig. 4. It is seen that the theoretical compliance corresponds closely to the experimental results when α and β are greater than unity. This indicates that the cantilever arms bend significantly beyond the crack tip and that the adhesive is deformed. Therefore it would be expected that the terms α and β could be related to the specimen dimensions and material properties of the adherends and adhesive (Mostovoy and colleagues, 1967); however this has not been attempted in the present study.

Fracture Toughness of Alumina Coatings

Fracture toughness values of alumina coatings which have been evaluated by this method are shown in Table 2. Cohesive failure occurs entirely within the coating whereas substrate-interfacial failure occurs at the interface between the substrate and coating. The term adhesive failure refers to failure between two plasma-sprayed coatings; such as a bond coat and a ceramic overlay. A major advantage of this method is that the crack path
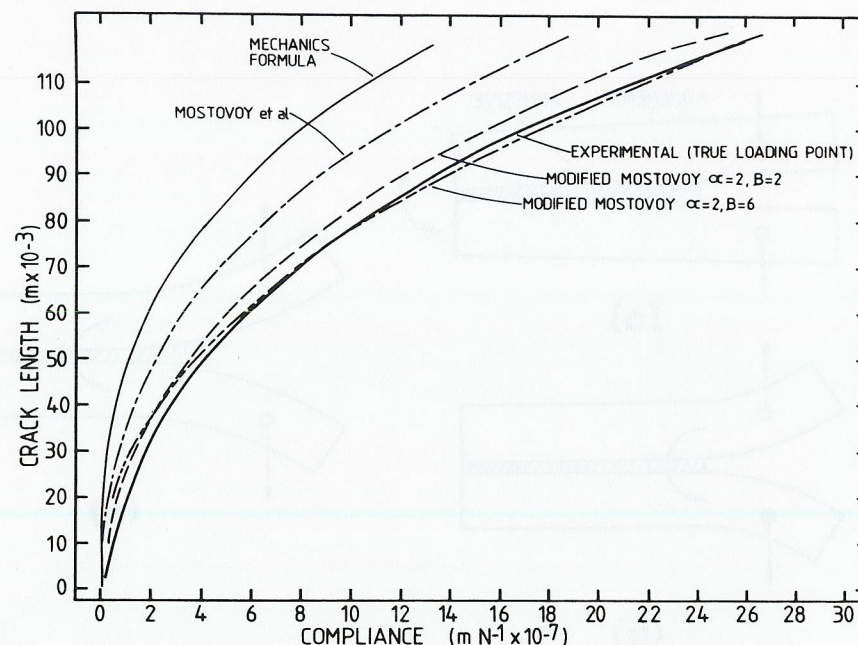

Fig. 4. Experimental compliance versus crack length functions compared to various theories.

TABLE 2. Fracture Toughness of Alumina Coatings

Failure Mode	G_{1C} range Jm^{-2}	G_{1C} mean Jm^{-2}	Standard Deviation
cohesive	16-27	21	5
substrate-interfacial (mild steel substrate)	10-15	12	2
adhesive (Ni-Al bond coat)	35-95	58	16

may be controlled by grooving of the DCB specimen to promote different failure modes. Other work, not reported here and in progress, concentrates on the fracture morphology of coatings and relates the adhesion strength value to the mechanism of cracking. The fracture mechanics technique presents a fundamental quantitative parameter related to coating adhesion which provides a more satisfactory basis for investigation of the mechanism of adhesion than the tests previously employed.

CONCLUSIONS

A fracture mechanics approach and verification of the testing technique have been outlined. Detailed analysis of the DCB compliance indicated that, in the case of these experiments, the loading conditions were soft. This decreases cracking stability and is clearly one experimental factor which can be changed to improve test reliability. The results indicate that the fracture mode may be controlled and that the various modes have distinctive strain energy release rates. This method provides a scientific means for examining the adhesion of plasma-sprayed coatings which is based on fundamental understanding of the adhesion mechanism.

ACKNOWLEDGEMENTS

REFERENCES

ASTM (1969). American Society for Testing and Materials. Standard C 633-69 Method of Test for Adhesion or Cohesive Strength of Flame-Sprayed Coatings.

Bascom, W. D. and J. L. Bitner (1977). A Fracture Approach to Thick Film Adhesion Measurements. J. Mater. Sci., 12, 1401-1410.

Becher, P. F. and W. L. Newell (1977). Adherence-Fracture Energy of a Glass-Bonded Thick-Film Conductor : Effect of Firing Conditions. J. Mater. Sci., 12, 90-96.

Berndt, C. C. and R. McPherson (1979). The Adhesion of Flame and Plasma Sprayed Coatings-A Literature Review. Australian Welding Research, 6, 75-85.

Berndt, C. C. and R. McPherson (1980). A Fracture Mechanics Approach to the Adhesion of Plasma Sprayed Coatings. Proc. 9th Int. Thermal Spraying Conf., May 12-23, 1980, pp.310-316, The Hague, Nederlands Instituut voor Lastechniek.

Berndt, C. C. and R. McPherson (1981). The Adhesion of Plasma Sprayed Ceramic Coatings to Metals. Mater. Sci. Research, 14, 619-628.

Clausing, D. P. (1969). Crack Stability in Linear Elastic Fracture Mechanics. Int. J. Fracture Mechanics, 5, 211-227.

Mostovoy,S., P. B. Crosley and E. J. Ripling (1967). Use of Crack-Line-Loaded Specimens for Measuring Plane-Strain Fracture Toughness. J. Materials, 2, 661-681.

Pabst, R.F. and G. Elssner (1980). Adherence Properties of Metal-to-Ceramic Joints. J. Mater. Sci., 15 188-196.

Rykalin, N. N. and V. V. Kudinov (1976). Plasma Spraying. Pure and Applied Chemistry, 48, 179-194.

Suhara, T., K. Kitajima and S. Fukada (1974). Coatings by Wire Explosion Spraying - Properties and Applications. Proc. 7th Inter. Metal Spraying Conf., Sept. 10th.-14th. 1973, pp.179-184, The Welding Institute, Cambridge, 1974.

Zakharov, B. M., M. G. Trofimov, L. I. Guseva, Yu. I. Golovkin, A. A. Kononov and V. V. Vinokurova (1970). Bond Strength of Coatings Applied by the Flame Plating Technique. Soviet Powder Metallurgy and Metal Ceramics, 9, 925-929.